

A Comparison of Plasma Performance Between Single-Null and Double-Null Configurations During ELMing H-mode

T.W. Petrie, M.E. Fenstermacher,¹ S.L. Allen,¹ T.N. Carlstrom, P. Gohil, R.J. Groebner, C.M. Greenfield, A.W. Hyatt, C.J. Lasnier,¹ R.J. La Haye, A.W. Leonard, M.A. Mahdavi, T.H. Osborne, G.D. Porter,¹ T.L. Rhodes,² D.M. Thomas, J.G. Watkins,³ W.P. West, N.S. Wolf, and the DIII-D Team

General Atomics, P.O. Box 85608, San Diego, California 92186-5608

¹Lawrence Livermore National Laboratory, Livermore, California

²University of California, Los Angeles, California

³Sandia National Laboratories, Albuquerque, New Mexico

Tokamak plasma performance generally improves with increased shaping of the plasma cross section, such as higher elongation and higher triangularity. The stronger shaping, especially higher triangularity, leads to changes in the magnetic topology of the divertor. Because there are engineering and divertor physics issues associated with changes in the details of the divertor flux geometry, especially as the configuration transitions from a single-null (SN) divertor to a marginally balanced double-null (DN) divertor, we have undertaken a systematic evaluation of the plasma characteristics as the magnetic geometry is varied, particularly with respect to (1) energy confinement, (2) the response of the plasma to deuterium gas fueling, (3) the operational density range for the ELMing H-mode, and (4) heat flux sharing by the divertors. To quantify the degree of “divertor imbalance” (or equivalently, to what degree the shape is “double-null” or “single-null”), we define a parameter DRSEP. DRSEP is taken as the radial distance between the upper divertor separatrix and the lower divertor separatrix, as determined at the outboard midplane. For example, if DRSEP=0, the configuration is a magnetically balanced DN; if DRSEP = +1.0 cm, the divertor configuration is biased toward the upper divertor. Three examples are shown in Fig. 1. In the following discussions, ∇B drift is directed toward the “lower” divertor. Parameters used in this experiment are given in Fig. 1.

SN characteristics are maintained over a wide range in DRSEP, *except* for DRSEP values near zero. Some aspects of this are shown by the “dynamic” DRSEP scan in Fig. 2. From $t = 2.0$ s to 3.4 s, the magnetic bias was toward the lower divertor [Fig. 2(b)], and Type-1 ELMs were present [Fig. 2(c)]. Total stored energy W_T [Fig. 2(d)], line-averaged density \bar{n}_e

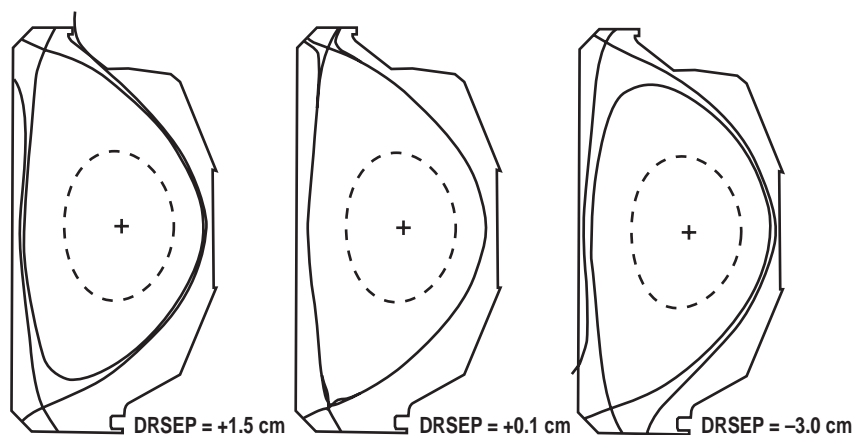


Fig. 1: Three of the plasma shapes considered in this study are shown: DRSEP= +1.5 cm (upper SN), DRSEP = +0.1 cm (near-balanced DN), and DRSEP = -3.0 cm (lower SN). The direction of the ∇B drift is toward the lower divertor. Plasma parameters: $I_p = 1.37$ MA, $B_T = 2.0$ T, $q_{95} = 4-5$, triangularity of the primary X-point = 0.78, $P_{input} = 4.5-7.0$ MW, $Z_{eff} = 1.7$, DRSEP = -4 cm to +4 cm. No active particle pumping at the divertor strike points or in the private flux region was done for these discharges.

and edge “pedestal” density [1] $n_{e,ped}$ [Fig. 2(e)] were nearly constant up to $t \approx 3.2$ s (or $DRSEP \approx -1$ cm) but increased after this time with the loss of the Type-1 ELMs. This discharge was in near-magnetic balance from $t \approx 3.4$ – 3.6 s but briefly reverted to a lower single-null configuration, producing a (transient) return to Type-1 ELMs. For $t \geq 4.0$ s, the magnetic configuration had become biased upward. When $DRSEP \approx +0.5$ cm, Type-1 ELMs reappeared and were maintained for the remainder of the shot. The energy confinement time reached its highest values for the DN characterized by -1.0 cm $< DRSEP < +0.5$ cm. The energy confinement times outside this range in DRSEP were reduced from the DN values, although still fairly high (i.e., $\tau_E/\tau_{E89P} \approx 2.8$ – 3.0 for peak “DN” operation and $\tau_E/\tau_{E89P} \approx 2.2$ – 2.4 for peak “SN” operation, where τ_E is the energy confinement time and τ_{E89P} refers to the 1989 ITER L-mode scaling [2]).

When DRSEP was fixed during a shot and deuterium gas was puffed, τ_E decreased, irrespective of the DRSEP value. In general, there were two distinct phases of plasma behavior during gas puffing. Figure 3 shows an example for a “lower” SN. Deuterium gas puffing ($\Gamma_{D2} = 60$ Torr ℓ/s) was started at $t = 3.25$ s and held constant thereafter [Fig. 3(b)]. Phase I, which covered approximately the first 0.5 s of gas puffing, was characterized by a drop in τ_E/τ_{E89P} , as well as a coincident drop in edge electron pressure [5] $P_{e,ped}$ [Fig. 3(c)]. Neither the line-averaged density \bar{n}_e nor the pedestal electron density $n_{e,ped}$ increased [Fig. 3(d)]. Phase II was characterized by a “plateau” in τ_E/τ_{E89P} (≈ 1.4); for our data set, τ_E/τ_{E89P} lay in the range 1.3–1.6 during the “plateau” phase. Note also that the “edge” or pedestal electron pressure was also constant and that steady fueling of the main plasma was coincident with the start of Phase II.

The confinement decrease was not limited to the edge plasma. We examined the radial profiles in density and temperature at three times for the shot shown in Fig. 3: (1) $t = 3.25$ s (at the start of deuterium puffing), (2) $t = 3.75$ s (start of Phase II), and (3) $t = 5.0$ s (well into the density rise during Phase II). The electron density profile was unchanged between 3.25 s and 3.75 s; steady fueling of the core plasma occurred only during Phase II. In Phase I both electron and ion temperatures decreased $\approx 30\%$ in the outer region of the main plasma ($\rho/a > 0.6$) and decreased $\approx 10\%$ – 25% in the interior regions. During Phase II both electron and ion temperatures continued to decrease across the radial profile, but (with the rise in electron density) the plasma pressure across the profile remained approximately constant in time.

At present, the reason for the degradation in τ_E and poor core fueling during Phase I is unclear. Transport analysis of the main plasma with the ONETWO [3] code has indicated that electron conductivity did not change appreciably during Phase I for $\rho/a < 0.7$. Ion conductivity, however, increased by about a factor of 2–4 across the profile during this time. While the electron conductivity inside the $q = 2$ flux surface was still considerably higher than the ion conductivity even after 400 ms of puffing, the ion conductivity rose to become comparable with electron conductivity outboard of the $q = 2$ surface. From this preliminary transport analysis, the initial decrease in energy confinement following the start of gas puffing appears

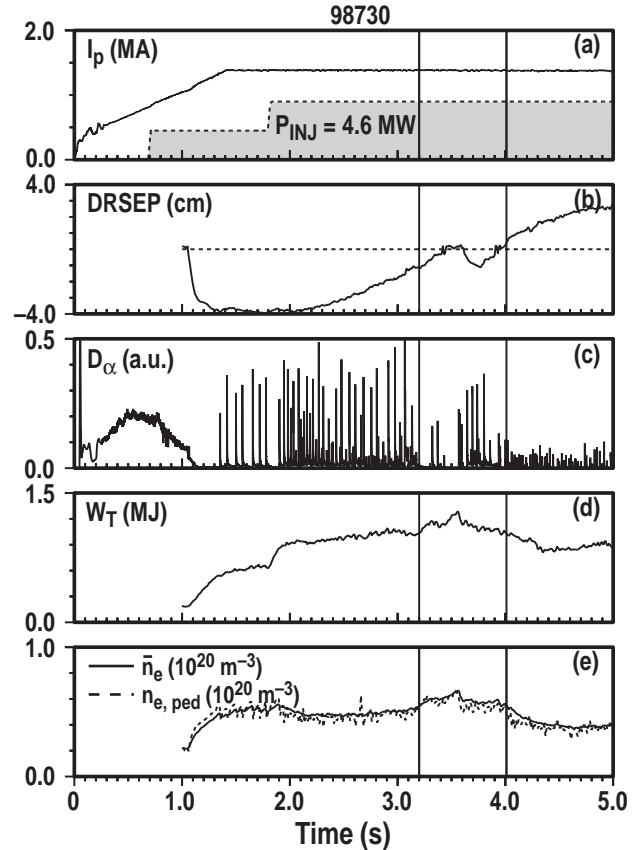


Fig. 2. The “dynamic” scan in DRSEP shows that small shifts away from $DRSEP = 0$ result in SN behavior. There was some variation in q_{95} between $t = 2.0$ and 5.0 s; between $t = 3.0$ and 4.2 s, $q_{95} = 4.7$ – 5.1 .

to be a consequence of increased ion transport. Analysis also has indicated that even before gas puffing, both electron and ion conductivity peaked sharply near the $q = 2$ flux surface. We might expect strong MHD activity (e.g., an $m/n = 3/2$ tearing mode) to be driving this transport increase. Our analysis, however, shows little MHD activity near $q = 2$ (e.g., $m/n = 3/2$). For this particular shot, there was also low amplitude $m/n = 4/3$ activity, which vanished just before the beginning of Phase II, but the spatial location of this activity was well inside the $q = 2$ surface and was likely not responsible for this increase in transport. Some MHD activity in the core plasma was present in all shots we investigated. In all shots there was $n = 1$ activity (sawtooth).

We define the H-L density limit as the line-averaged density at which the discharge loses ELMy characteristics and distinctive edge density gradient. Figure 4 (which normalizes the H-mode density limit to the Greenwald limit [4]) shows an H-mode density limit dependence on DRSEP. While there does not appear to be a pronounced variation between $DRSEP = -3.5$ cm and 0.0, the normalized density limit dropped 15%–20% between 0.0 cm and +1.0 cm.

The peak heat flux under either outboard divertor is a strong function of magnetic (im)balance between $DRSEP = -1$ cm and +1 cm. This is shown in Fig. 5(a). The data, through which we have drawn hyperbolic tangent function, are not symmetric with respect to $DRSEP=0$. The “peak heat flux balance” point is $\approx +0.2$ cm. At the “magnetic balance” point (i.e., $DRSEP=0$), Fig. 5(a) implies that the peak heat flux to the “lower” divertor is approximately twice that of the peak heat flux to the “upper” divertor.

Detailed fitting of the heat flux profiles to an exponential function indicates that the scrape-off length ($\lambda_{q_{\parallel}}$) of the parallel heat flux at the outboard midplane also has a DRSEP-variation. This is shown in Fig. 5(b); the squares represent $\lambda_{q_{\parallel}}$ determined by an infrared camera monitoring the lower divertor and the circles determined by an infrared

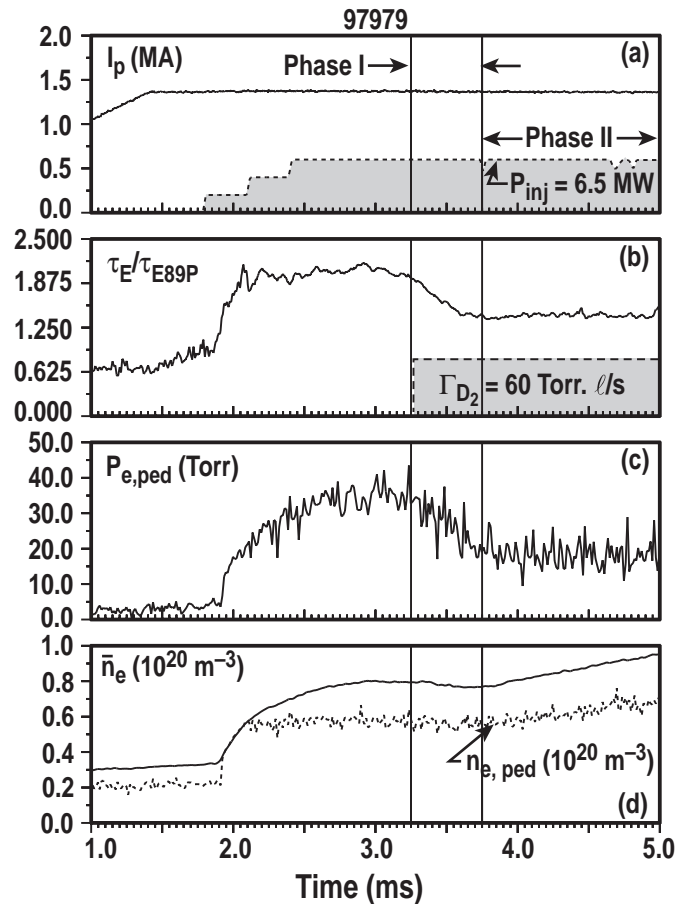


Fig. 3. Deuterium gas is injected into a lower SN divertor plasma, starting at $t = 3.25$ s. $DRSEP = -3.7$ cm. Phase I: Electron energy confinement degrades with little rise in density. Phase II: Energy confinement is stable and density rises.

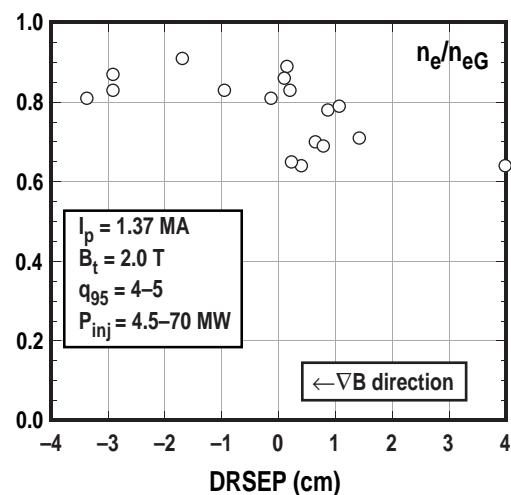


Fig. 4. The H-mode density limit changes measurably between $DRSEP = 0$ and 1.5 cm. The density is normalized to the Greenwald density limit.

camera monitoring the upper divertor. For $DRSEP < 0$, $\lambda_{q_{\parallel}} \approx 0.6$ cm. Our analysis shows, however, that $\lambda_{q_{\parallel}}$ had a minimum between $DRSEP = 0$ and 1 cm, and increases afterward as $DRSEP$ becomes more positive.

When $\lambda_{q_{\parallel}}/|DRSEP| \ll 1$, $\lambda_{q_{\parallel}}$ defined by the primary (or main) separatrix is little affected by the existence of the separatrix of the secondary divertor. However, we speculate that when $DRSEP$ is roughly equal to $\lambda_{q_{\parallel}}$, the secondary separatrix begins to truncate the profile of q_{\parallel} , as power flow is siphoned to the secondary divertor and the power profile gains in steepness (implying a smaller $\lambda_{q_{\parallel}}$). The shift in the minimum from $DRSEP=0$ might be expected, because of the relative strength in the peak heat flux of the lower divertor when magnetically-balanced.

We have found that gas puffing degraded the energy confinement of these high triangularity ELMing discharges to levels where $\tau_E/\tau_{E89L} \approx 1.3-1.6$. This appeared to be true, regardless of the $DRSEP$ value. When this energy confinement “plateau” was reached, continued gas puffing had a much less deleterious effect on confinement and particle fueling. For these unpumped plasmas, we have not been able to fuel an ELMing H-mode plasma to higher density with gas puffing only, and simultaneously maintain an energy confinement of $\tau_E/\tau_{E89P} \approx 2$. (Recent experiments where pumping the private flux region were done during gas puffing, however, did yield high confinement ($\tau_E/\tau_{E89P} \approx 2$) and densities at or above the Greenwald limit for “lower” SN divertors.)

We have noted advantages to operating in the DN and near-DN configuration, such as better energy confinement and more efficient fueling. Our data, however, indicate that the presence of ELMs is sensitive to $DRSEP$, when $DRSEP$ falls in the range -1 cm to $+1$ cm, i.e., within $\approx (1-2) \lambda_{q_{\parallel}}$. This sensitivity to $DRSEP$ near zero was also observed in other important properties, such as H-mode operating density range and divertor heat flux sharing. On the other hand, the behavior of these properties in cases where one or the other X-point was dominant (i.e., commonly referred to as “SN”) was rather insensitive to variation in $DRSEP$, at least between $DRSEP = -4$ and -1 cm (i.e., “lower” SN) and between $DRSEP = +1$ cm and $+4$ cm (i.e., “upper” SN). Thus, if the balanced DN is the preferred configuration, adequate control over $DRSEP$ is essential.

This is a report of work supported by the U.S. Department of Energy under Contract Nos. DE-AC03-99ER54463, W-7405-ENG-48, DE-AC04-94AL85000, and Grant No. DE-FG03-86ER53225.

- [1] R.J. Groebner and T.H. Osborne, Phys. Plasmas **5** (1998) 1800.
- [2] P.N. Yushmanov, et al., Nucl. Fusion **30** (1990) 1999.
- [3] W.W. Pfeiffer, “ONETWO: A Computer Code For Modeling Plasma Transport in Tokamaks,” General Atomics Report GA-A16178 (1980).
- [4] M. Greenwald, et. al., Nucl. Fusion **28** (1988) 2199.
- [5] L.L. Lao, et. al., Nucl. Fusion **25** (1985) 1611.
- [6] C.J. Lasnier, et. al., Nucl. Fusion **38** (1998) 1225.

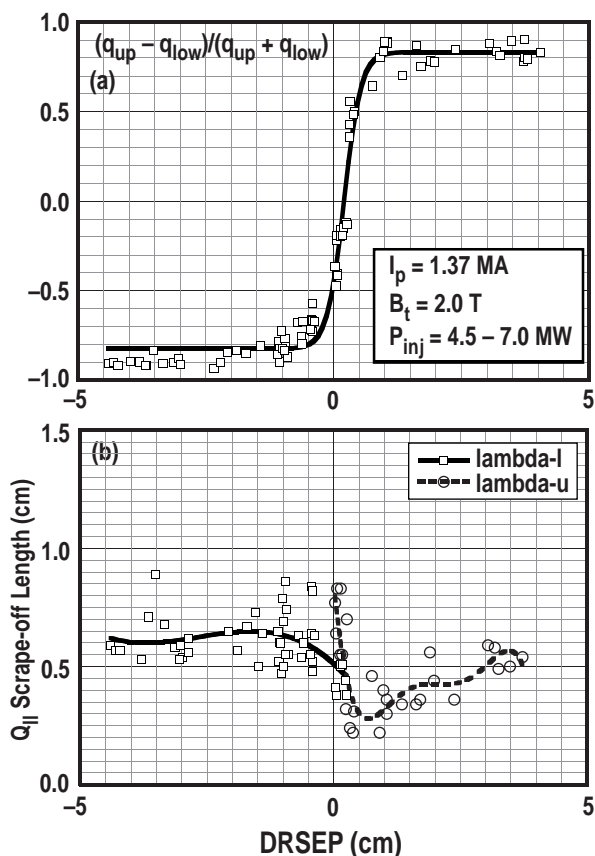


Fig. 5. (a) Peak heat flux is roughly a factor of 2 higher in the “lower” divertor, when the configuration is in magnet balance. The peak heat flux is balanced when $DRSEP \approx 0.25$ cm. Uncertainty in $DRSEP < 0.2$ cm. (b) A variation in $\lambda_{q_{\parallel}}$ occurred between $DRSEP = 0$ and 1 cm. Infrared camera data from the lower (\square) and upper (\circ) divertor are used. Polynomial fits to each dataset are shown. The scrape-off profiles at the midplane are found by projecting the heat flux distribution from the divertors back to the midplane using the EFITD [5] magnetic reconstruction code and the VIDDAPS [6] heat flux analysis code.